

Spectral Broadening and Suppression of Excitation Induced by Ultralong-Range Interactions in a Cold Rydberg Atom Gas

Kilian Singer, Markus Reetz-Lamour, Thomas Amthor, Luis Gustavo Marcassa,^y and Matthias Weidemüller^z
 Physikalisches Institut der Universität Freiburg, Hermann-Herder-Str.3, 79104 Freiburg, Germany^x
 (Dated: May 23, 2019)

We report on the observation of ultra long-range interactions in a gas of cold Rubidium Rydberg atoms. The van-der-Waals interaction between a pair of Rydberg atoms separated as far as 100,000 Bohr radii features two important effects: Spectral broadening of the resonance lines and suppression of excitation with increasing density. The density dependence of these effects is investigated in detail for S-, P- and D-Rydberg states with main quantum numbers $n = 60$ and $n = 80$ excited by narrow-band continuous-wave laser light. The spectral broadening of the P-states is compared to ab initio interaction potentials. The density-dependent suppression of excitation can be interpreted as the onset of an interaction-induced local blockade.

PACS numbers: 32.80.Rm, 32.80.Pj, 34.20.Cf, 03.67.Lx

With the advances in laser cooling and trapping techniques, new intriguing perspectives for the investigation of Rydberg atoms [1] have been opening. When cooled to very low temperatures, the core motion can be neglected for the timescales of Rydberg excitation ("frozen Rydberg gas"). Unexpected effects have been discovered, such as the many-body division of excitation [2, 3], the population of high-angular-momentum states through free charges [4], or the spontaneous formation and recombination of ultracold plasmas [5, 6]. Other fascinating features of cold, interacting Rydberg atoms have been proposed but not been observed so far, including the creation of ultralong-range molecules [7, 8], whereas molecular crossover resonances have already been found experimentally [9]. One of the most outstanding properties of Rydberg atoms is their high polarizability, caused by the large distance between the outer electron and the core. Rydberg atoms are thus very sensitive to electric fields and are expected to exhibit strong long-range dipole-dipole and van-der-Waals (vdW) interactions. First indications of interaction effects between Rydberg gases at high densities have been found in an atomic beam experiment [10] and recent collisional evidence for ultralong-range interactions in a Rydberg gas has been reported [11]. In a frozen gas these interactions make Rydberg atoms possible candidates for quantum information processing [12, 13]. One promising approach is based on the concept of a dipole blockade [13], i.e. the inhibition of multiple Rydberg excitations in a confined volume due to interaction-induced energy shifts.

In this Letter we report on experimental evidence for ultralong-range interactions in a frozen Rydberg gas, which are interpreted as the onset of the dipole blockade, and we present high-resolution spectroscopic signa-

tures of these interactions. Similar indications of suppressed excitation have recently been observed in pulsed Rydberg excitation from a cold gas [14]. In contrast to these findings, our experiment makes use of a tunable narrow-bandwidth continuous-wave (cw) laser for Rydberg excitation and thus allows for high-resolution spectroscopy of the resonance lines. By varying the density of Rydberg atoms the influence of interactions on the strength and the shape of these lines is investigated in detail. Interaction-induced features in both the broadening of the lines and saturation of the resonance peak height are observed.

To realize a frozen gas of Rydberg atoms we trap about 10^7 ^{87}Rb atoms in a dispenser-loaded magneto-optical trap (MOT). The MOT is located inside a vacuum chamber (background pressure 5×10^{-11} mbar) which consists mainly of a spherical cube with good optical access along the three main orthogonal axes and the two diagonals. The MOT coils are located inside the vacuum chamber. The trapping laser light is provided by a diode laser system consisting of two diode lasers which are simultaneously injection-locked to a frequency-stabilized extended cavity diode laser (ECDL) at 780 nm and added coherently [15]. The output of this laser-addition setup is sent through a single-mode optical fiber for mode-cleaning providing about 70 mW at the output. The frequency is detuned by 1.5 (natural line width $\Delta = 6.1 \text{ MHz}$) to the red of the cooling and trapping transition ($5S_{1/2}; F=2 \rightarrow 5P_{3/2}; F=3$). A second ECDL drives the repumping transition ($5S_{1/2}; F=1 \rightarrow 5P_{3/2}; F=2$).

Both laser beams are split and directed through the three main axes of the spherical cube creating a cloud of atoms with a $1-e^2$ -diameter of 1.2 (0.2) mm at a temperature of 100 K.

The laser light for driving the transition to Rydberg states ($5P_{3/2}; F=3 \rightarrow 5P_{1/2}$) is provided by a commercial laser system (Toptica, TA-SHG 110) consisting of an ECDL at 960 nm subsequently amplified to 1 W and then frequency doubled to 479 nm with a line width $< 2 \text{ MHz}$. The output beam which can be switched by an acousto-optical modulator (AOM) is guided along one of the diag-

^x Electronic address: kilian.singer@physik.uni-freiburg.de

^y Instituto de Física de São Paulo, Caixa Postal 369, 13560-970, São Carlos, São Paulo, Brazil

^z Electronic address: m.weidemuller@physik.uni-freiburg.de

^x URL: <http://quantendynamik.physik.uni-freiburg.de>

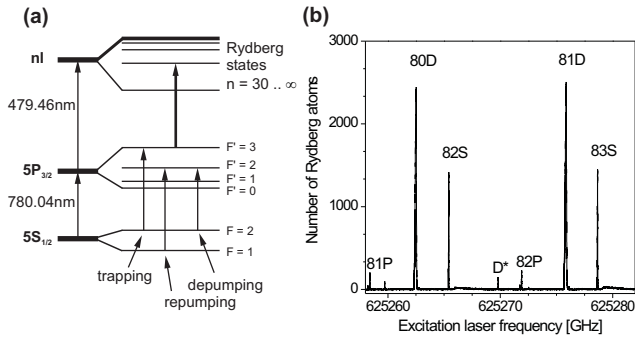


FIG. 1: (a) Relevant energy levels of ^{87}Rb . Indicated are the transitions driven by the trapping laser, the repumping and the depumping lasers at 780 nm, and the Rydberg excitation laser at 479 nm. (b) Typical Rydberg spectrum at $n = 80$ taken with a reduced intensity of the blue laser ($100 (15) \text{ W/cm}^2$). Besides the two dipole allowed S and D states, the dipole forbidden P states are also excited due to residual electrical fields. The small D* line is attributed to a hyperfine excited from the ground state.

onalkes of our vacuum chamber and focused to a waist of $80 (10) \text{ } \mu\text{m}$ at the center of the atom cloud. The Rydberg atoms are field-ionized by applying a voltage of 40 Volts to the central field plates consisting of nickel meshes separated by 13.2 mm with 95% transparency through which the MOT beams pass almost unperturbed. The ions are accelerated onto a micro-channel plate detector (MCP). Residual electrical fields during Rydberg excitation are mainly caused by the MCP potential of -1.9 kV . Field components perpendicular to the field plates are compensated by applying a small voltage, while parallel field components are measured to be less than 0.16 V/cm .

The excitation into Rydberg states is schematically shown in Fig. 1(a). At the beginning of an excitation cycle, the trapping laser is tuned into resonance. After 15 s, the blue Rydberg excitation laser which is tuned to the $n' = 60$ and $n' = 80$ Rydberg manifold is switched on for 20 s. Since the lifetime of the Rydberg states is much longer, Rydberg atoms are accumulated during this time interval. The trapping laser is then reset to the MOT detuning of -1.5 , and an electric field of 27 V/cm is applied to ionize the Rydberg atoms. The excitation cycle is repeated every 20 ms while maintaining a continuously loaded steady-state MOT. To take an excitation spectrum, the frequency of the blue laser is repetitively scanned at a rate of typically 300 MHz/s .

The density of Rydberg atoms can be varied by changing the population of atoms in the $5\text{P}_{3/2}; F = 3$ state. This is accomplished by depopulating the $5\text{S}_{1/2}; F = 2$ state into the $5\text{S}_{1/2}; F = 1$ state in a controlled way. For this purpose, the repumping laser is attenuated by an AOM while an additional depumping laser resonant with the transition $5\text{S}_{1/2}; F = 2 \rightarrow 5\text{P}_{3/2}; F = 2$ (see Fig. 1(a)) is switched on. Within 1 ms, the density of atoms in the $5\text{P}_{3/2}$ state is lowered by one order of magnitude as is measured by recording the fluorescence at

780 nm with a photodiode. During this short period of time, the size of the atom cloud remains unaltered. Due to the two-step Rydberg excitation scheme, the variation in the $5\text{P}_{3/2}$ density is directly transformed into a change of the number of excited Rydberg atoms, since the excitation volume is defined by the overlap of the blue laser beam with the atom cloud remains fixed. Absolute numbers of Rydberg atoms per excitation cycle are obtained by comparing the number of atoms lost from the trap, as deduced from the change of fluorescence rate at 780 nm, with the integrated ion signal. In the same manner, the nonlinear response of the MCP at large ion signals can be calibrated. Throughout this paper, the number of Rydberg atoms is derived from the number of measured ions at the MCP after calibration. Due to the uncertainty in determination of the MOT size and density, we estimate the systematic error for the absolute number of Rydberg atoms to be a factor of 2 while the values for Rydberg peak densities are uncertain within a factor of roughly 3.

A Rydberg spectrum for $n = 80$ is depicted in Fig. 1(b). About 2500 Rydberg atoms are detected for the strong dipole-allowed D transitions. The resonance line width is typically 30 MHz caused by saturation broadening of the first excitation step. Dipole-forbidden P states are also excited due to the residual electrical field. Under our experimental conditions, the ion formation rate for $n = 80$ states through blackbody radiation [1] is estimated from calculated lifetimes [16] to be approximately 200 Hz . Ionization rates due to collisions of cold Rydberg atoms with residual hot Rydberg atoms are of the same order of magnitude assuming an upper limit of 10^8 cm^{-3} for the densities of hot Rydberg atoms. We therefore do not expect significant effects of spontaneous creation of ions and avalanche processes during the timescales of excitation (20 s) [5].

To study interaction effects between Rydberg atoms, spectra at different Rydberg densities are taken. The density is changed by either varying the power of the excitation laser or by changing the density of atoms in the $5\text{P}_{3/2}$ state, as described above. In Fig. 2(a) the resonance line for the $82\text{S}_{1/2}$ peak is shown at different Rydberg densities. Fig. 2(a1) and 2(a2) are taken at low intensity of the blue excitation laser ($I = 6 \text{ W/cm}^2$) and at $5\text{P}_{3/2}$ densities of $0.4 \cdot 10^9 \text{ cm}^{-3}$ and $2.5 \cdot 10^9 \text{ cm}^{-3}$, respectively. In this 'low excitation regime', the line shows no broadening. In addition, the number of excited Rydberg atoms on resonance scales linearly with the $5\text{P}_{3/2}$ density. The behavior changes drastically when the intensity of the blue excitation laser is increased to 500 W/cm^2 . Figs. 2(a3) and (a4) show the resonance line at $5\text{P}_{3/2}$ densities of $0.3 \cdot 10^9 \text{ cm}^{-3}$ and $2.0 \cdot 10^9 \text{ cm}^{-3}$, respectively. In the 'high excitation' regime characterized by Rydberg densities of the order 10^8 cm^{-3} , one observes an asymmetric broadening of the line which can be attributed to level shifts of Rydberg states induced by the long-range vdW interactions of Rydberg atom pairs excited from $5\text{P}_{3/2}$ atoms at a mean distance of 10 m . Similar broadening effects have been observed earlier in

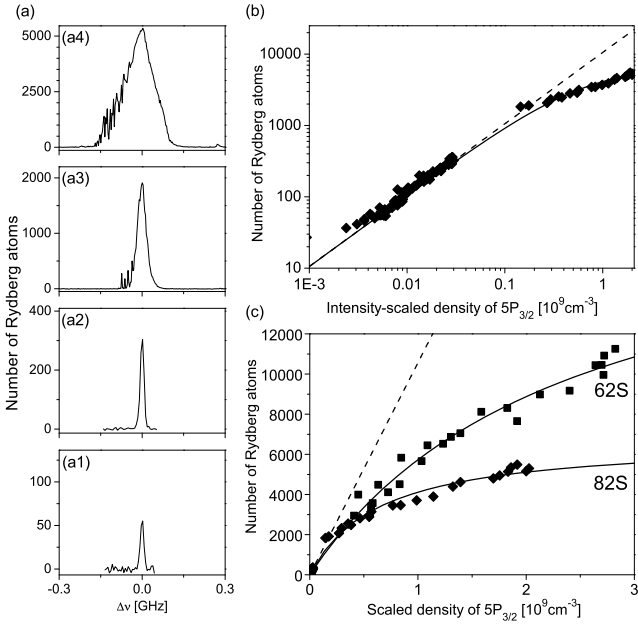


FIG. 2: (a) $82S_{1=2}$ resonance line for different excitation rates and $5P_{3=2}$ densities. For details see text. (b) $82S_{1=2}$ resonance peak height versus scaled $5P_{3=2}$ density. The $5P_{3=2}$ density at low intensity is scaled with the ratio of the intensities. The solid line shows a fit to a saturation function, while the dashed line gives a linear extrapolation from the initial slope. (c) Comparison of the $82S_{1=2}$ and $62S_{1=2}$ peak heights on resonance. For $62S_{1=2}$ the abscissa is scaled by $I_{62S} = I_{82S}$ ($n_{82S} = n_{62S}$)³ = 1:7 (see text). Solid and dashed lines as in (b).

an atomic beam experiment [10]. However, due to our high-resolution approach in a cold gas, we detect these effects at densities four orders of magnitude lower.

The line broadening is accompanied by an excitation suppression on resonance. At maximum excitation rate and density, we detect only 5000 Rydberg atoms on resonance, which is a factor of 4 lower than expected from simple linear density and excitation intensity scaling. To further clarify this point, we have plotted the number of Rydberg atoms excited on resonance versus the scaled $5P_{3=2}$ density in Fig. 2(b). If no interaction was present and the transition is not saturated, we expect the numbers of Rydberg atoms to scale as $N_{Ryd} / n_{5P} I (n)^3$, with I being the intensity of the excitation laser and n the main quantum number corrected by the corresponding quantum defect [1]. Therefore we connect the low and high intensity data by introducing an intensity-scaled density $n_{5P} = n_{5P} I = I_{high}$. As can be seen in Fig. 2(b) both data sets can be smoothly connected by a heuristic saturation function for the number of Rydberg atoms of the form $N_{Ryd} = N_0 \frac{n_{5P} = n_{sat}}{1 + n_{5P} = n_{sat}}$. A fit to the data yields $N_0 = 6700$ atoms and $n_{sat} = 0.6 \cdot 10^9 \text{ cm}^{-3}$. We have carefully ruled out saturation of our MCP detector, and thus attribute the saturation of the Rydberg excitation to interatomic interactions leading to the onset of

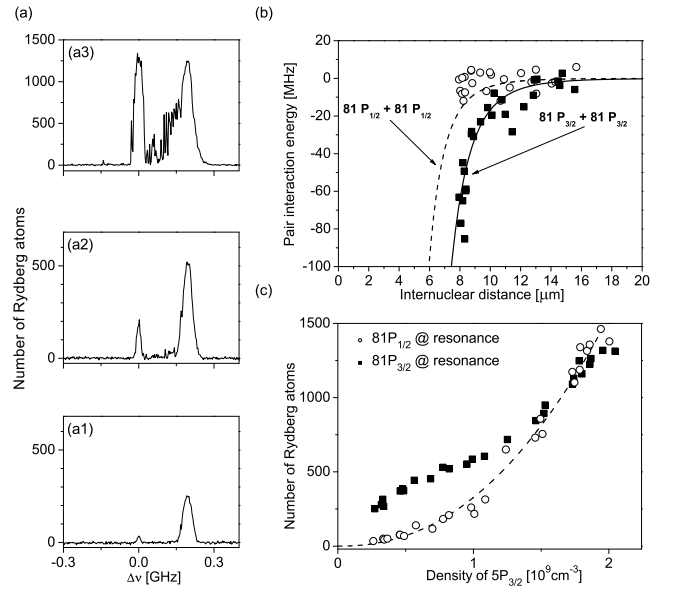


FIG. 3: (a) Resonance line for the fine structure doublet $81P_{1/2}$ (left) and $81P_{3/2}$ (right) at different densities of the $5P_{3=2}$ state. (b) Van-der-Waals pair potentials (dashed line: $81P_{1/2} + 81P_{1/2}$ asymptote, solid line: $81P_{3/2} + 81P_{3/2}$ asymptote) versus the internuclear distance. The dots show the experimental data for the effective line broadening (circles: $81P_{1/2}$, squares: $81P_{3/2}$). (c) Resonance peak height of the $81P_{1/2}$ and the $81P_{3/2}$ line as a function of $5P_{3=2}$ density.

a dipole blockade [13, 14]. In contrast to the original proposal based on resonant dipole-dipole interaction, the blockade is caused by vdW interaction in our case.

To further test this interpretation we have compared the saturation for different main quantum numbers n . As the vdW interaction potential between two Rydberg atoms scales with n^{11} , one expects much weaker saturation for lines with lower main quantum number, although the transition strength of these lines is much stronger. Fig. 2(c) shows a comparison of resonantly excited Rydberg atoms on the $82S_{1=2}$ and the $62S_{1=2}$ line. While the data for the $82S_{1=2}$ excitation are identical to Fig. 2(b), the $5P_{3=2}$ density for the $62S_{1=2}$ excitation is scaled as previously described: $n_{5P} = n_{5P} (I_{62S} = I_{82S}) (n_{82S} = n_{62S})^3$. The solid lines show a fit with the same saturation function as described above. Within the experimental uncertainties and the fitting accuracy, both saturation curves yield the same slope at small values of the scaled density n_{5P} , while the saturation density of the $62S_{1=2}$ line is larger by a factor of 4 than the saturation density of the $82S_{1=2}$ line. Accordingly, the asymptotic number of Rydberg atoms for infinite density differs by a factor of 3. Similar results are obtained by comparing excitations to 80D and 60D levels. Although we are currently lacking a detailed model to describe the observed line shapes, all our findings qualitatively confirm the interpretation of a vdW blockade as the cause of the density dependent saturation.

The density dependence of the dipole-forbidden ne structure doublet $81P_{1=2}$ (left peak) and $81P_{3=2}$ (right peak) is depicted in Fig. 3(a). The graphs (a1) to (a3) are taken at $5P_{3=2}$ densities of $0.3 \cdot 10^9 \text{ cm}^{-3}$, $0.7 \cdot 10^9 \text{ cm}^{-3}$, and $1.9 \cdot 10^9 \text{ cm}^{-3}$, respectively. Two features are remarkable: With increasing density the $81P_{3=2}$ peak develops a wing on the red side of the resonance, while the $81P_{1=2}$ peak is hardly broadened, but grows much faster with density. The different broadening of the lines can be explained by the different vdW potentials experienced by the two ne structure components. In contrast to the S and D lines, theoretical predictions of the pair potentials are available [17, 18]. In Fig. 3(b) the attractive asymptotes of the vdW potentials are plotted versus the mean internuclear distance of atoms in the $5P_{3=2}$ state. We have extracted the interaction potential from the spectral line broadening of the red wings by subtracting the line width at low density from the observed widths of the red wings. Assuming a two-photon pair excitation from a $5P_{3=2} + 5P_{3=2}$ pair to be responsible for the line broadening [10], the resulting frequency width is multiplied by a factor of two. The data nicely fit the predicted interaction potentials for a maximum $5P_{3=2}$ density of about $2 \cdot 10^9 \text{ cm}^{-3}$ consistent with the experimental value.

In contrast to the dipole-allowed S and D lines, the dipole-forbidden $81P_{1=2}$ and $81P_{3=2}$ peaks grow much faster than linear with $5P_{3=2}$ density, as shown in Fig. 3(c). A fit to the data of the $81P_{1=2}$ resonance yields a scaling with $n_{5P}^{2.0(1)}$. The behavior of the $81P_{3=2}$ peak is more complicated, but shows saturation relative to the $81P_{1=2}$ peak, which may again be caused by a similar interaction-induced blockade effect as discussed above. Whether the density dependence of the dipole-forbidden P lines may be attributed to interaction-induced S- and D-attractions has to be clarified in the framework of a detailed model for the cw Rydberg excitation in a cold gas which is under development.

In conclusion, we have explored signatures of a strongly interacting, cold Rydberg gas, revealing measurable effects over interatomic distances as large as 100,000 Bohr radii. The interaction shows up in two distinct effects: A broadening of resonance lines by the pair-interaction

vdW potential, and a suppression of on-resonance excitation. We find good agreement between the observed broadening with predicted interaction potentials in the case of the $81P$ ne-structure doublet. Theoretical calculations of the S- and D-interaction potentials are underway, which will allow for a more quantitative description of the observed line shapes. Thus the high spectroscopic resolution that we achieve constitutes a precise direct determination of long-range interaction potentials. The saturation of Rydberg excitation with increasing density constitutes a complementary signature of the ultra long-range Rydberg-Rydberg interactions and marks the onset of a vdW-induced dipole blockade.

While the spectral broadening of the resonance lines can only be understood as an "instantaneous" excitation of Rydberg pairs, it remains to be clarified whether the density-dependent saturation occurs in a similar way or whether it is induced by an avalanche-like process based on the successive creation of Rydberg atoms. The latter hypothesis has successfully been employed in the interpretation of similar saturation effects recently observed for Rydberg atoms excited through short duration, high intensity laser pulses from a cold gas [14]. Our unique spectroscopic resolution provides important experimental information to further elucidate the processes underlying the dipole blockade. Our experimental approach employing narrow-band cw Rydberg excitation can directly be applied to the implementation of quantum information processing with Rydberg atoms [13, 19] by further increasing the density, thus proceeding from the two-body limit to the full many-body regime of the dipole blockade.

The project is supported in part by the Landesstiftung Baden-Württemberg in the framework of the "Quantum Information Processing" program. We acknowledge contributions from Simon Fölling and Michaela Scherneck in the early phase of the experiment. We are also indebted to Dirk Schwalm for generous support when the experiment was started at the Max-Planck-Institute for Nuclear Physics. We thank Robin Côte, Philip Gould and Ed Eyler for valuable discussions and providing us with the $81P$ potentials. The collaboration with L.G.M. is supported by the PROBRAL program of the DAAD.

[1] T. F. Gallagher, *Rydberg Atoms* (Cambridge University Press, Cambridge, 1994).

[2] I. Mourachko et al., *Phys. Rev. Lett.* **80**, 253 (1998).

[3] R. C. Stoneman et al., *Phys. Rev. Lett.* **58**, 1324 (1987).

[4] S. Dutt et al., *Phys. Rev. Lett.* **86**, 3993 (2001).

[5] M. Robinson et al. (2000).

[6] T. F. Gallagher et al., *J. Opt. Soc. Am. B* **20**, 1091 (2003).

[7] C. H. Greene et al., *Phys. Rev. Lett.* **85**, 2458 (2000).

[8] C. Boisseau et al., *Phys. Rev. Lett.* **88**, 133004 (2002).

[9] S. Farooqi et al., *Phys. Rev. Lett.* **91**, 183002 (2003).

[10] J. Rainond et al., *J. Phys. B: At. Mol. Phys.* **14**, L655 (1981).

[11] A. L. de Oliveira et al., *Phys. Rev. Lett.* **30**, 143002 (2003).

[12] D. Jaksch et al., *Phys. Rev. Lett.* **85**, 2208 (2000).

[13] M. D. Lukin et al., *Phys. Rev. Lett.* **87**, 037901 (2001).

[14] D. Tong et al., *arXiv:physics/0402113* (2004).

[15] K. Singer et al., *Opt. Comm.* **218**, 371 (2003).

[16] C. E. Theodosiou (2000), *priv. comm.*

[17] R. Côte, *priv. comm.*

[18] M. Mărinescu, *Phys. Rev. A* **56**, 4764 (1997).

[19] B. K. Teo et al., *Phys. Rev. A* **68**, 053407 (2003).